PFC/JA-87-2

Particle Confinement Improvement During 2.45GHz Lower-Hybrid Current Drive Experiments

M.J. Mayberry, K-I. Chen, S.C. Luckhardt, M. Porkolab

January 1987

Plasma Fusion Center
Massachusetts Institute of Technology
Cambridge, Massachusetts 02139 USA

This work was supported by DOE Contract No. DE-AC02-78ET-51013.

Submitted for publication to Physics of Fluids.

Particle Confinement Improvement During 2.45 GHz Lower-Hybrid Current Drive Experiments

M.J. Mayberry,[a] K-I. Chen, S.C. Luckhardt, M. Porkolab
Plasma Fusion Center
Research Laboratory of Electronics
and
Department of Physics
Massachusetts Institute of Technology
Cambridge, Massachusetts 02139

Abstract

Particle confinement behavior during 2.45 GHz lower-hybrid current drive has been investigated on the Versator II tokamak. It is found that during combined Ohmic and rf current drive the global particle confinement time, τ_p, increases by up to a factor of two compared to purely Ohmically driven discharges, as observed in earlier 800 MHz experiments at lower densities $\overline{n}_e \leq 6 \times 10^{12}\,\mathrm{cm}^{-3}$ [Phys. Fluids **29**, 1985 (1986)]. In the present experiments, τ_p increases have been observed at densities up to $\overline{n}_e = 2 \times 10^{13}\,\mathrm{cm}^{-3}$.

[a] Present Address: GA Technologies Inc., San Diego, CA 92138.

Density increases have been observed previously in a number of tokamak experiments in which lower-hybrid current drive has been combined with inductive ohmic heating to maintain or increase the plasma current.[1-4] Such density increases can result from three possible causes: 1) increased ionization of hydrogen (due to an increase in particle recycling), 2) increased influx of impurities, or 3) an increase in the particle confinement time. In previous Versator II 800 MHz experiments[5] it was shown that the density increases observed during rf current drive were due to a factor-of-two increase in the global particle confinement time, τ_p, compared to purely ohmically driven discharges. However, because of the low rf source frequency used in those experiments, the confinement investigations were restricted to the relatively low-density regime below the density limit for current drive ($\overline{n}_e < 6 \times 10^{12}\,\mathrm{cm}^{-3}$).[1]

We report here on recent particle confinement studies carried out during 2.45 GHz lower hybrid current drive experiments. As reported previously,[6,7] with the higher rf source frequency, plasma current increases, loop voltage drops and enhancements in the nonthermal electron cyclotron emission have been observed at densities up to $\overline{n}_e \simeq 2 \times 10^{13}\,\mathrm{cm}^{-3}$, approximately a factor of three higher than the 800 MHz density limit. At a line-averaged density of $\overline{n}_e \simeq 1.3 \times 10^{13}\,\mathrm{cm}^{-3}$, factor-of-two increases in τ_p have been observed during the injection of 65 kW of 2.45 GHz rf power, compared to purely ohmically driven plasmas. The τ_p improvement increases linearly with the 2.45 GHz rf power, until the maximum line-averaged density during the rf pulse approaches $\overline{n}_e \simeq 2 \times 10^{13}\,\mathrm{cm}^{-3}$. Above this density, 2.45 GHz current drive effects become negligibly small, and the particle confinement improvements also disappear.

The experiments were carried out on the Versator II tokamak ($R = 40.5\,\mathrm{cm}$, $a = 13\,\mathrm{cm}$, $B_t \leq 15\,\mathrm{kG}$, $I_p = 30 - 40\,\mathrm{kA}$). Lower-hybrid slow waves were excited in the plasma using a stainless steel four-waveguide-array antenna, mounted on an outside port of the tokamak. The individual waveguide dimensions were: 1.0 cm width, 8.64 cm height, 0.15 cm wall thickness. With a relative waveguide phasing of $+\pi/2$, the calculated Brambilla power spectrum of the antenna ranges from $N_\parallel = ck_\parallel/\omega = 1$ to $N_\parallel = 5$, with 75% of the total power launched in the direction of the electron ohmic drift velocity. With the 2.45 GHz rf system, quasi-steady-state fully rf-driven discharges have been achieved at densities up

to $\overline{n}_e = 1 \times 10^{13}\,\mathrm{cm}^{-3}$.[6] At higher densities, flat-topping the plasma current has not been possible due to insufficient rf power available ($P_{rf} \leq 95\,\mathrm{kW}$). Therefore, in order to study the global particle confinement properties of rf current-driven plasmas at high densities, we have injected rf power into ohmically sustained plasmas, comparing the global particle confinement of the plasma immediately before and during the rf injection. For all the data presented, the rf pulse length ($7-10\,\mathrm{ms}$) was long compared to the estimated bulk particle confinement time ($1-2\,\mathrm{ms}$).

The typical density behavior during ohmically heated discharges with and without rf injection is shown in Fig. 1. The gas feed rate, controlled with a piezoelectric puff valve, was held constant during the entire time interval shown. The line-averaged density before the rf firing time at $t = 20\,\mathrm{ms}$ is $\overline{n}_e = 1.1 \times 10^{13}\,\mathrm{cm}^{-3}$. Without rf, the density remains nearly constant. In contrast, when 65 kW of rf power is injected with $+\pi/2$ waveguide phasing, the density rises by nearly a factor of two, to $\overline{n}_e = 2.0 \times 10^{13}\,\mathrm{cm}^{-3}$. The density typically starts to rise approximately 1 ms after the beginning of the rf pulse. Once the maximum value is reached, in this case 6 ms later, sawtooth oscillations with slow-rise and fast-fall characteristics appear on the density trace. During the remainder of the rf pulse, the density decays slightly or remains constant, depending on the in/out plasma motion. Following the termination of the rf pulse, however, the density always decays rapidly.

The ionization rate of hydrogen is determined from the brightness of the H_α line emission. For the plasma conditions in these experiments, the H_α emissivity is proportional to the volumetric hydrogen ionization rate.[8] As shown in Fig. 1, the H_α brightness level measured near the edge of the plasma decreases during the density rise. In the ohmic discharge, with the same rate of gas feed, the H_α brightness level remains nearly constant. The maximum reduction in the H_α brightness level during the rf pulse is approximately 30%. Note, however, that once the density reaches its maximum level of $\overline{n}_e = 2.0 \times 10^{13}\,\mathrm{cm}^{-3}$, the H_α emission quickly returns to its original level.

The behavior of impurity species was also monitored during rf injection using the VUV monochrometer. As shown in Fig. 1, the brightness of the O V impurity line (emitted from the outer region of the plasma) remains constant during the first 7 ms of the rf pulse, during the density rise. Once the density maximum is reached, however, the O V brightness

increases slightly. Other impurity lines surveyed, including C V (emitted near the plasma center) and C III (emitted near the edge) exhibit similar temporal behavior. We conclude from these measurements that the observed density rise during current drive cannot be due to an influx of impurities, nor to an increase of hydrogen ionization, but rather to an improvement in the global particle confinement time τ_p. A quantitative estimate of the τ_p increase requires spatial profile measurements of the density and the H_α emission.

The global particle balance equation is given by:

$$\tau_p = \frac{N_e}{S - dN_e/dt}, \tag{1}$$

where N_e is the total number of electrons, and S is the total ionization source term. The total number of electrons is given by the volume integral of the density profile,

$$N_e(t) = 4\pi^2 R \int_0^a r n_e(r,t)\, dr, \tag{2}$$

where $n_e(r,t)$ is obtained from Abel-inverted 4 mm interferometer data. The H_α emission was monitored at various times from three different toroidal locations. Two available tangential side ports afforded a direct view of the limiter and the rf antenna. A third port, located below the tokamak, was used for radial scans of the plasma cross section. The time dependence of the H_α signal was approximately the same at each toroidal location. Hence, following Ref. 5, we have assumed that the temporal evolution of S is independent of the toroidal location, deducing relative changes in S from the Abel-inverted H_α profile measurements. The ionization source term is then given by:

$$S(t) \propto \int_0^a r E_\alpha(r,t)\, dr, \tag{3}$$

where it has been assumed that the H_α emissivity, E_α, is proportional to the volumetric hydrogen ionization rate.[8] The source term $S(t)$ is then normalized, using Eq. (1), by choosing a reasonable value for τ_p just prior to rf injection which is consistent with the observed density behavior in Ohmic discharges.

Abel-inverted profiles of the density $n_e(r)$ and the H_α emissivity $E_\alpha(r)$ are shown in Fig. 2. The line-averaged density just before the rf injection ($t = 19$ ms) is $\overline{n}_e = 1.3 \times$

$10^{13}\,\mathrm{cm}^{-3}$. As the density rises during the rf pulse to a maximum of $\overline{n}_e = 1.9 \times 10^{13}\,\mathrm{cm}^{-3}$, the density profile steadily broadens. This is in contrast to the low density 800 MHz experiments on Versator[5] where the density profile become more peaked during rf injection. The H_α emissivity profile, which is localized to the outer region of the plasma cross section, remains nearly unchanged.

The time histories of N_e, S and τ_p shown in Fig. 3 are very similar to those measured in the earlier 800 MHz experiments.[5] While the total number of electrons in the plasma increases by 50%, the total ionization source term decreases by more than 30%. Hence, the global particle confinement time τ_p, calculated from Eq. (1), increases by a factor of two during the 2.45 GHz rf pulse. The improvement in τ_p appears to saturate and even decline somewhat as the line averaged density rises to a level near $\overline{n}_e = 2 \times 10^{13}\,\mathrm{cm}^{-3}$.

The particle confinement improvement during 2.45 GHz current drive varies with the injected rf power level as shown in Fig. 4. In this power scan the initial density was $\overline{n}_e = 1.3 \times 10^{13}\,\mathrm{cm}^{-3}$. With $+\pi/2$ current drive phasing, the rise in the density, $\Delta\overline{n}_e$, and the drop in the H_α brightness increase linearly with the rf power level, except at the highest power levels where the effects begin to saturate. The global particle confinement time estimated from these density and H_α measurements shows a similar behavior, increasing with the applied rf power level until $\Delta\overline{n}_e$ becomes so large that the line-averaged density exceeds $\overline{n}_e = 1.8 \times 10^{13}\,\mathrm{cm}^{-3}$. The saturation effect could be due to the increase in the injected rf power level, or to the increase in density. It is interesting to note, however, that the saturation of τ_p coincides with the reduction of other current drive effects at densities near $\overline{n}_e \simeq 2 \times 10^{13}\,\mathrm{cm}^{-3}$. For two of the data points shown in Fig. 4, the antenna phasing was reversed to $\Delta\phi = -\pi/2$, such that the waves were launched in the anti-current drive direction. In these cases, the increase in τ_p was less than half of that obtained with $+\pi/2$ phasing at a comparable power level.

The dependence of the density rise during the rf pulse, $\Delta\overline{n}_e$, on the target plasma density level just prior to rf injection is shown in Fig. 5. The rf power level was in the range $P_{rf} = 60 - 70\,\mathrm{kW}$, except at the lowest densities where it was reduced slightly in order to avoid excessive outward plasma motion caused by large rf induced current increases. As shown in Fig. 5, the density rise during rf injection can be as large as a

factor of two when the initial density is sufficiently low ($\overline{n}_e \leq 1 \times 10^{13}\,\mathrm{cm}^{-3}$). At higher densities, the effects become smaller. There also appears to be an upper density limit for improved particle confinement. For a toroidal field strength of 11 kG, this limit occurs at a density of $\overline{n}_e \simeq 2.1 \times 10^{13}\,\mathrm{cm}^{-3}$. Below this limit, density rises are accompanied by decreases in the H_α emission. Above the limit, slight density decreases are observed, accompanied by small increases in the H_α emission. These latter observations indicate that the bulk particle confinement may actually be degraded by the rf at the higher densities. A similar transition in particle confinement behavior was observed at the upper density limit for strong wave-electron interaction ($\bar{n}_c \simeq 5 \times 10^{13}\,\mathrm{cm}^{-3}$) on the FT tokamak,[9] where a 2.45 GHz rf frequency was used as well. As shown in Fig. 5, when the toroidal field strength is lowered from 11 kG to 9 kG, the density rise observed during rf injection is substantially reduced. In addition, the upper density limit for improved particle confinement decreases to $\overline{n}_e \simeq 1.5 \times 10^{13}\,\mathrm{cm}^{-3}$. This dependence on the toroidal magnetic field suggests that poor wave accessibility may be responsible for the upper density limit for improved τ_p during 2.45 GHz current drive. Note that at the interception points ($\Delta\overline{n}_e = 0$), $\omega_{pe}^2(0)/\omega_{ce}^2(0) \simeq 2.6$, a relatively high value of the dielectric constant.

From our results, it appears that the improvement in global particle confinement observed during 2.45 GHz lower hybrid current drive is due to the rf generation of a quiescent superthermal electron tail. The dependences of τ_p on rf power, antenna phasing and plasma density resemble those of other current drive effects observed such as the incremental current increase[7] and the nonthermal cylotron emission[6] (see Fig. 1). We note that in the earlier 800 MHz experiments at low densities, τ_p improvements were observed during current drive only when a relaxation instability of the fast electron tail due to the anomolous doppler effect[10] was suppressed by the injection of sufficient rf power levels. Under certain conditions, the threshhold power level required for complete tail mode suppression was as low as 4 kW. However, increasing the rf power level well above this threshhold produced no further improvement in τ_p, despite significant increases in the rf-driven current. For all the 2.45 GHz data presented here, the level of plasma hard x-ray emission prior to the rf injection was negligible, indicating that few energetic ($E > 20\,\mathrm{keV}$) electrons were present. In addition, there was no evidence of bursting rf emission either before or during the rf pulse which would signify tail mode oscillations. Improvements in τ_p scaled linearly with

the rf power level, with no evidence of a power thresshold. Despite these contrasts, the following conclusion appears to be consistent with the results from both experiments: the generation of a *quiescent* superthermal electron tail with lower hybrid waves is correlated with an improvement in the global particle confinement.

In order to explain the factor-of-two density increases observed in either experiment, a mechanism which links the presence of a stable superthermal electron tail to bulk particle confinement must be established. Possible candidates include: 1) a reduction in magnetic fluctuations due to suppression of MHD activity during current drive, 2) a modification of the electrostatic potential profile of the plasma, and 3) a reduction in low frequency drift wave activity. So far, we have investigated only the first of these possibilities. Preliminary measurements of the MHD activity during current drive have been carried out using $\dot{B}_\theta$ loops to measure poloidal field fluctuations and a gas-filled proportional counter to measure soft x-ray fluctuations. Typically, during the period of density rise, the level of poloidal field fluctuations appears to decrease as indicated by a reduction in the amplitude of the $\dot{B}_\theta$ signal. Once the density reaches the maximum level, however, the poloidal field fluctuations return to their original level. Also at this time, the sawtooth oscillations appear on the density trace as well as on the soft x-ray signal from the center of the plasma. While these effects may indicate a change in the MHD behavior, it is not known whether this is the cause of the sudden degradation in particle confinement when the density reaches $\overline{n}_e \simeq 2 \times 10^{13}\,\mathrm{cm}^{-3}$ (see the H_α trace in Fig. 1). More detailed studies of the MHD activity during current drive are clearly warranted.

In summary, we have studied the particle confinement behavior during combined ohmic/LHCD discharges with a 2.45 GHz source frequency. This has allowed us to investigate lower-hybrid current drive at relatively high densities ($\overline{n}_e > 8 \times 10^{12}\,\mathrm{cm}^{-3}$), and to extend the density regime over which improved particle confinement was obtained in earlier 800 MHz experiments. During lower hybrid current drive, the particle confinement time increases typically by a factor of two with 65 kW of rf injection and $\Delta\phi = +\pi/2$ waveguide phasing. The τ_p increases observed during rf injection disappear at densities above $\overline{n}_e \simeq 2 \times 10^{13}\,\mathrm{cm}^{-3}$, where other current drive effects also diminish. At these densities, $\omega_{pe}^2(0)/\omega_{ce}^2 \geq 2$, and the accessibility of low-$N_\parallel$ waves, which are the most efficient in

driving current, is expected to be severely restricted. Although the particle confinement improvement appears to be correlated with the amount of rf driven current, further investigations will be required to determine the physical mechanism linking the generation of a fast electron tail to bulk plasma confinement.

Acknowledgments

This work was supported by the U. S. Department of Energy under Contract No. DE-AC02-78ET-51013.

References

1. S.C. Luckhardt, M. Porkolab, S.F. Knowlton, K-I. Chen, A.S. Fisher, F.S. McDermott, M.J. Mayberry, Phys. Rev. Lett. **48**, 152 (1982).

2. K. Ohkubo, S. Takamura, and the JIPPT-II Group, *Proceedings of the 3rd Joint Varenna-Grenoble International Symposium on Heating of Toroidal Plasmas*, edited by C. Gormezano, G.G. Leotta, and E. Sindoni (Commission of the European Communities, Brussels, 1982), Vol. 2, p. 543.

3. G. Tonon, G. Gormezano, C. Cardinalli, M. El Shaer, W. Hess, G. Ichtchenko, R. Maone, G. Melin, D. Moreau, G.W. Pacher, H.D. Pacher, F. Soeldner, and J.G. Wegrowe, *Proceedings of the 3rd Joint Varenna-Grenoble International Symposium on Heating of Toroidal Plasmas*, edited by C. Gormezano, G.G. Leotta, and E. Sindoni (Commission of the European Communities, Brussels, 1982), Vol. 2, p. 623.

4. K. Uehara and T. Nagashima, *Proceedings of the 3rd Joint Varenna-Grenoble International Symposium on Heating of Toroidal Plasmas*, edited by C. Gormezano, G.G. Leotta, and E. Sindoni (Commission of the European Communities, Brussels, 1982), Vol. 2, p. 485.

5. S.C. Luckhardt, K-I. Chen, M.J. Mayberry, M. Porkolab, Y. Terumichi, G. Bekefi, F.S. McDermott, R. Rohatgi, Phys. Fluids **29**, 1985 (1986).

6. M.J. Mayberry, M. Porkolab, K-I. Chen, A.S. Fisher, D. Griffin, R.D. Kaplan, S.C. Luckhardt, J. Ramos, R. Rohatgi, Phys. Rev. Lett. **55**, 829 (1985).

7. M.J. Mayberry, M. Porkolab, K-I. Chen, R.D. Kaplan, S.C. Luckhardt, R. Rohatgi, *Radiofrequency Plasma Heating (Sixth Topical Conference, Callaway Gardens, GA, 1985)*, edited by D.G. Swanson (American Institute of Physics, New York, 1982), p. 162.

8. L.C. Johnson and E. Hinnov, J. Quant. Spectrosc. Radiat. Transfer **13**, 333 (1973).

9. V. Pericoli-Ridolfini, Plasma Phys. and Controlled Fusion **27**, 709 (1985).

10. V.V. Parail and O.P. Pogutse, Nucl. Fusion **19**, 785 (1979).

Figure Captions

Fig. 1. Traces showing the temporal evolution of the line-average density, H_α brightness, O V impurity line brightness, and the $2\omega_{ce}$ emission during ohmically heated discharges with and without 2.45 GHz rf injection. In both cases the gas feed rate was fixed during the entire time interval shown.

Fig. 2. Abel-inverted density and H_α emissivity profiles before and during rf injection. The line-averaged density rises from $\overline{n}_e = 1.3 \times 10^{13}\,\mathrm{cm}^{-3}$ just before rf injection ($t = 19\,\mathrm{ms}$) to a maximum level during the rf pulse of $\overline{n}_e = 1.9 \times 10^{13}\,\mathrm{cm}^{-3}$ at $t = 26.5\,\mathrm{ms}$.

Fig. 3. Temporal evolution of the total electron number N_e, the ionization source term S, and the global particle confinement time τ_p calculated from the profiles of Fig. 2.

Fig. 4. Density rise $\Delta\overline{n}_e$, H_α brightness level, and global particle confinement time versus the rf power level for an initial density of $\overline{n}_e = 1.3 \times 10^{13}\,\mathrm{cm}^{-3}$ and $\Delta\phi = +\pi/2$ (current drive phasing). Also shown are two points (triangles) with the waveguide phasing reversed to $\Delta\phi = -\pi/2$.

Fig. 5. Dependence of the density rise during rf injection, $\Delta\overline{n}_e$, on the density of the ohmic target plasma just prior to the rf injection.

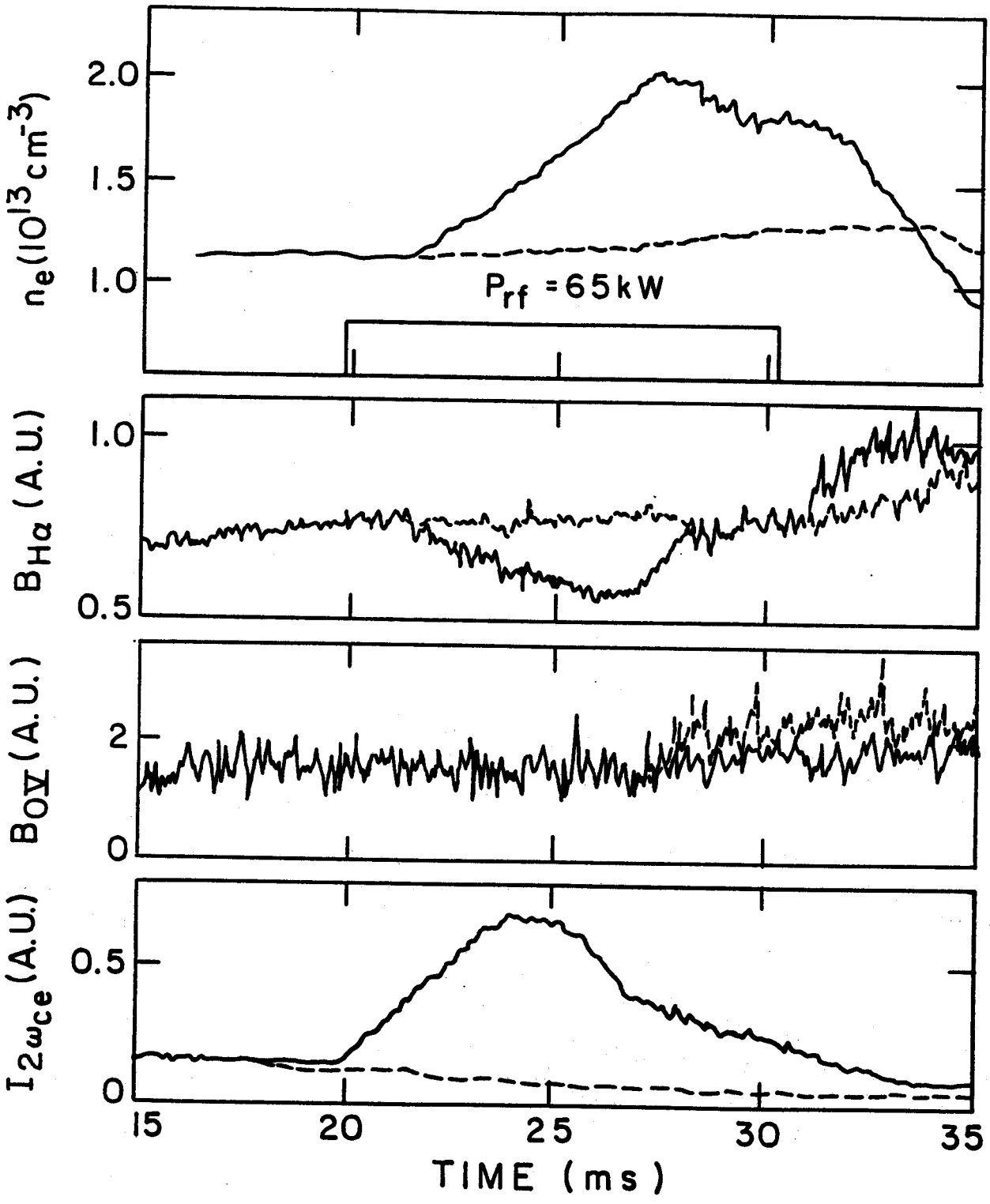
$n_e(10^{13}cm^{-3})$
2.0
1.5
1.0
P_{rf} = 65 kW
$B_{H\alpha}$ (A.U.)
1.0
0.5
B_{OV} (A.U.)
2
0
$I_{2\omega_{ce}}$ (A.U.)
0.5
0
15
20
25
30
35
TIME (ms)

Fig. 1

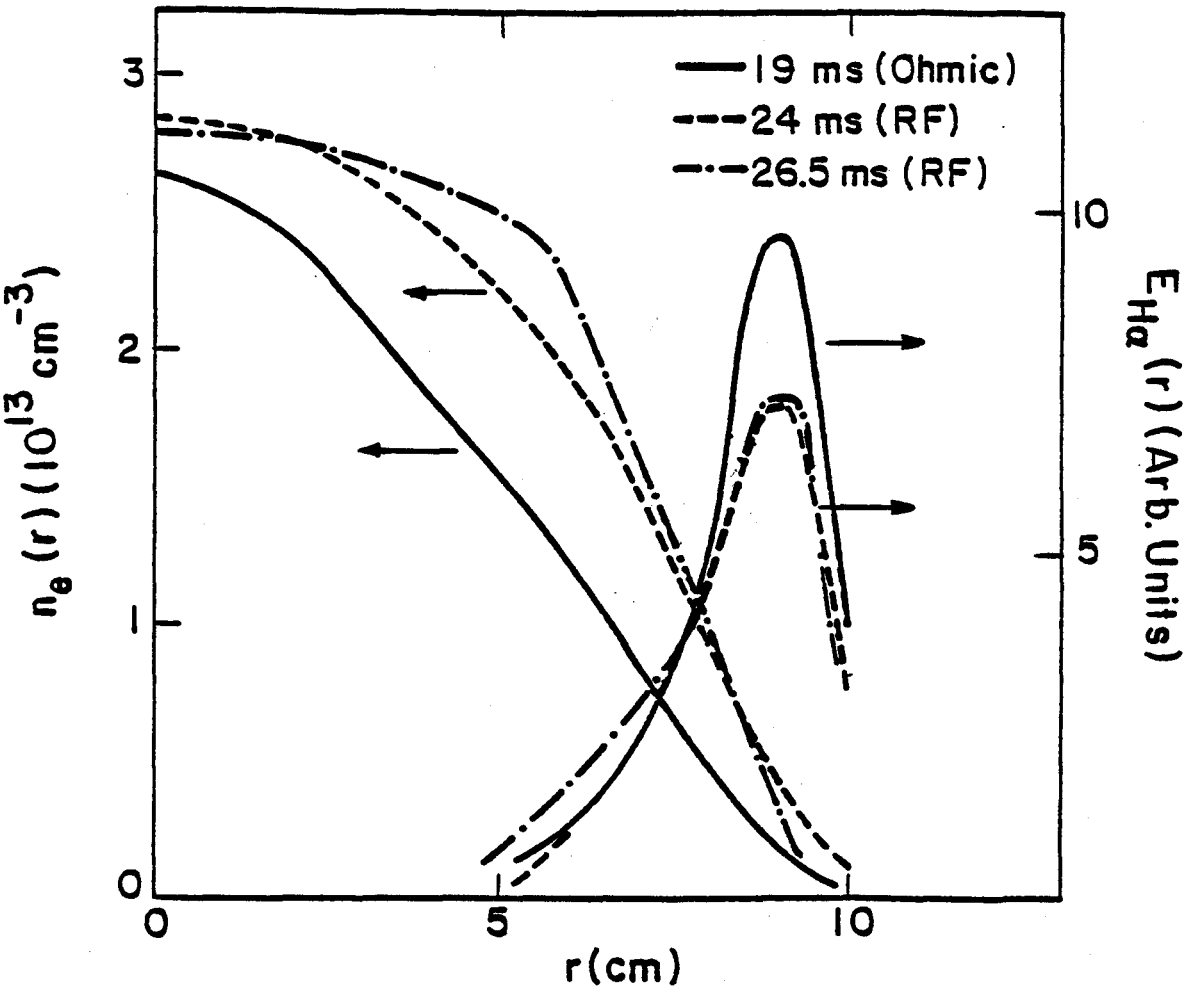
19 ms (Ohmic)
24 ms (RF)
26.5 ms (RF)
$n_e(r)\,(10^{13}\,cm^{-3})$
$E_{H\alpha}(r)$ (Arb. Units)
r(cm)
0
1
2
3
5
10

Fig. 2

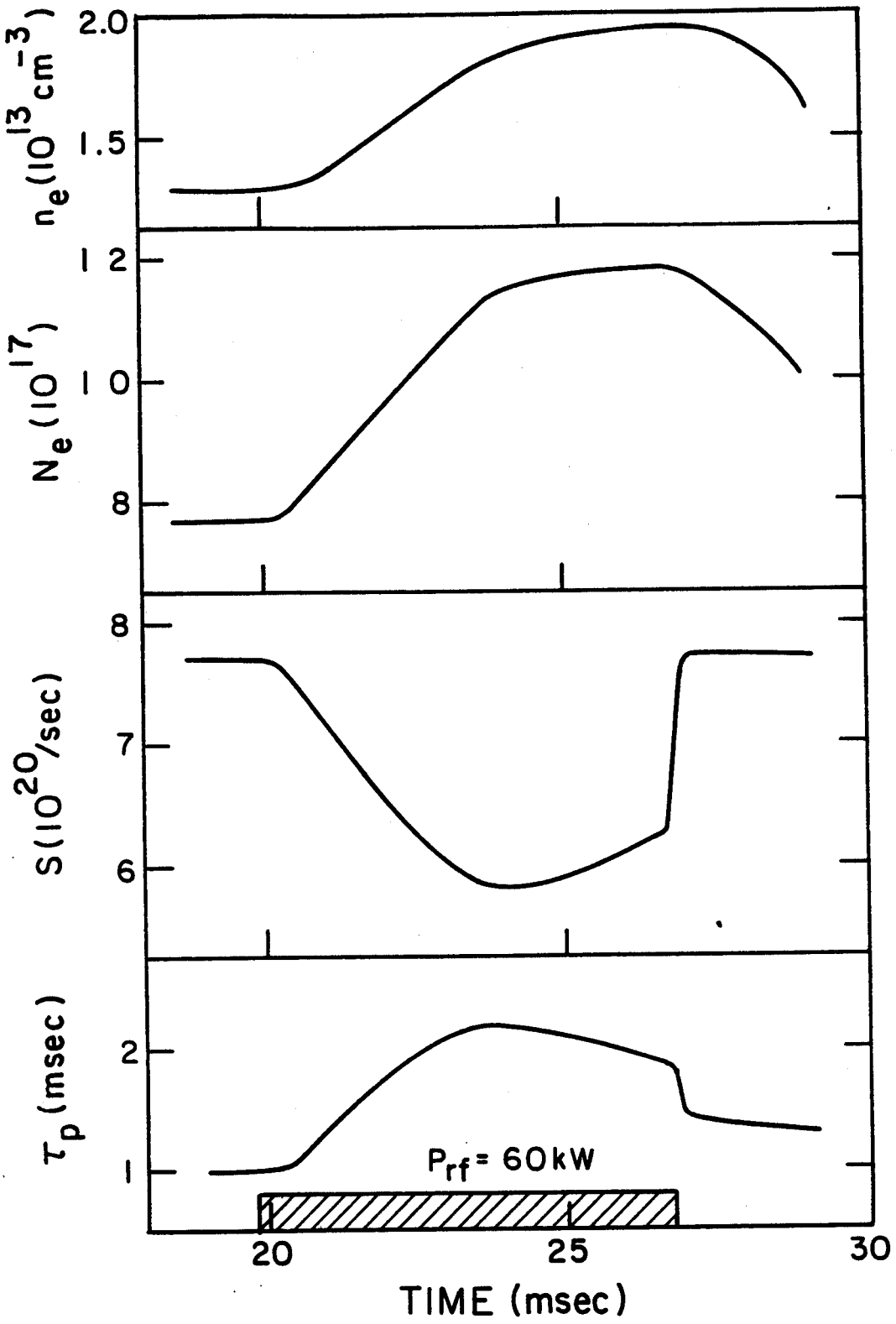
2.0
1.5
$n_e(10^{13}cm^{-3})$
1 2
1 0
8
$N_e(10^{17})$
8
7
6
$S(10^{20}/sec)$
2
1
τ_p (msec)
P_{rf} = 60kW
20
25
30
TIME (msec)

Fig 3

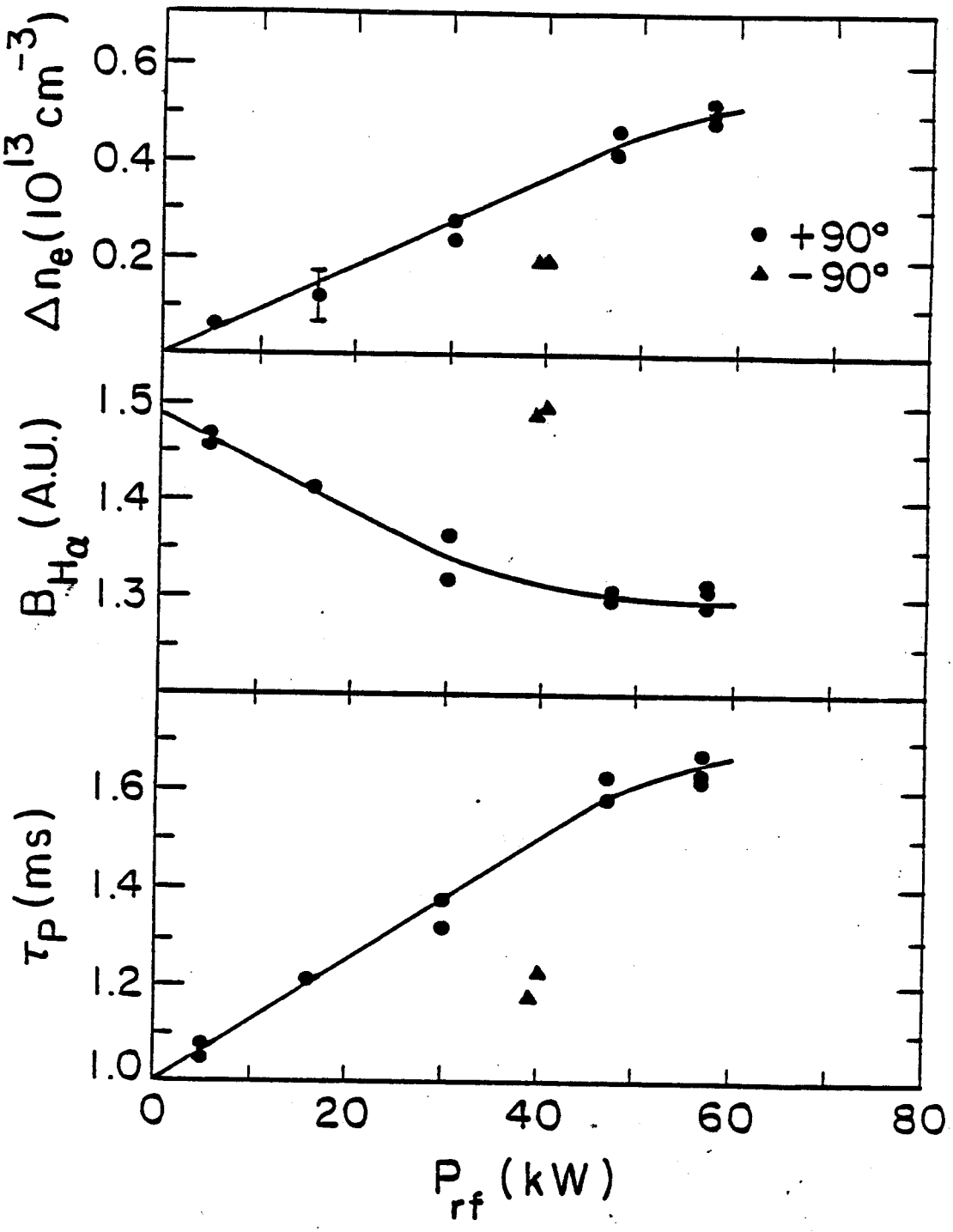
$\Delta n_e (10^{13} cm^{-3})$
0.6
0.4
0.2
+90°
−90°
B_{H_α} (A.U.)
1.5
1.4
1.3
τ_p (ms)
1.6
1.4
1.2
1.0
0
20
40
60
80
P_{rf} (kW)

Fig. 4

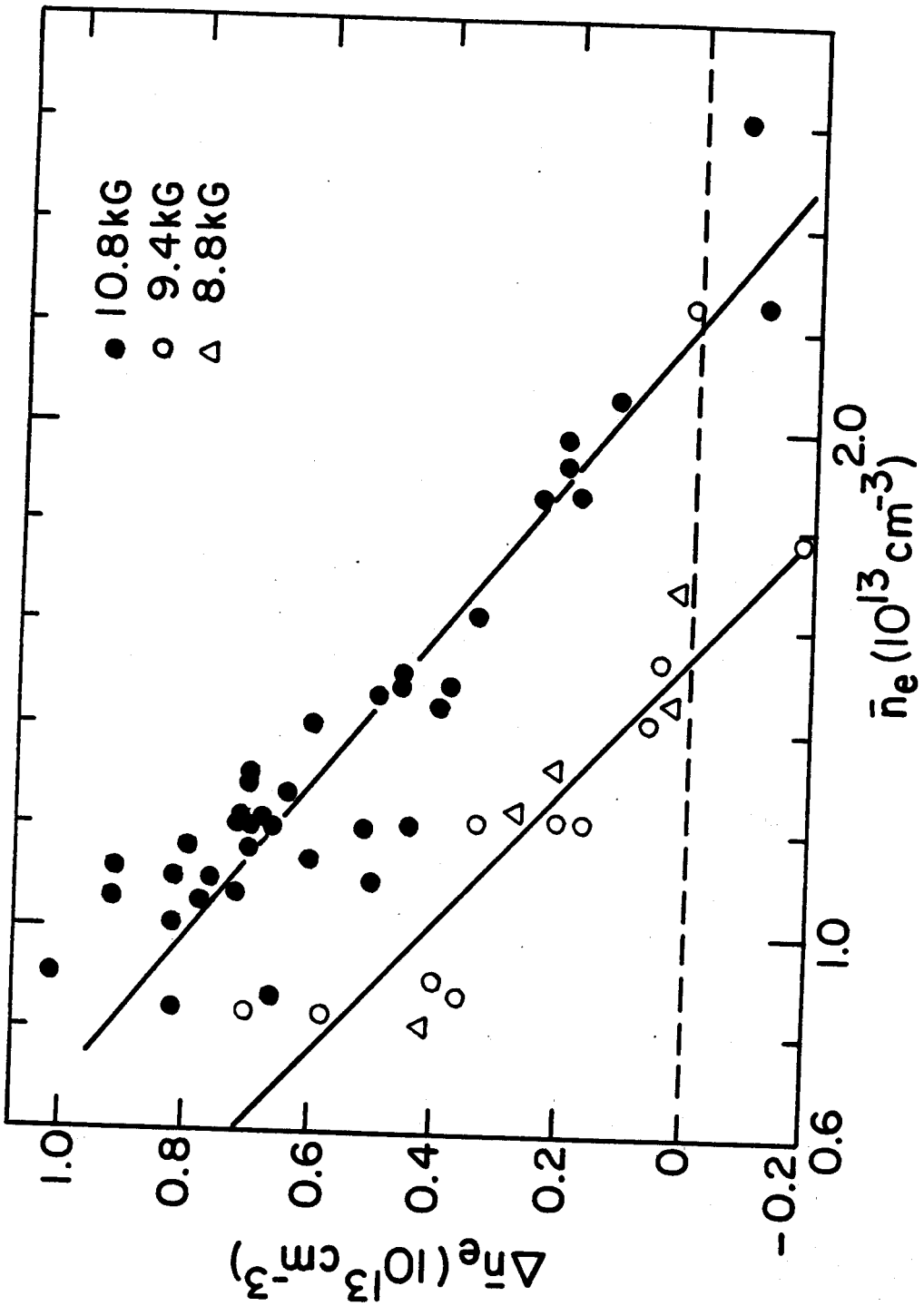
10.8kG
9.4kG
8.8kG
$\Delta\bar{n}_e$ (10^{13} cm^{-3})
$\bar{n}_e$ (10^{13} cm^{-3})
1.0
0.8
0.6
0.4
0.2
0
-0.2
0.6
1.0
2.0

FIG. 5